

Growth, structure, and magnetic properties of Fe monolayers on $\text{Cu}_{84}\text{Al}_{16}(100)$

M. D. Martins, L. H. F. Andrade, P. L. Gastelois, and W. A. A. Macedo^{a)}

Laboratório de Física Aplicada, Centro de Desenvolvimento da Tecnologia Nuclear, CP 941, 30123-970 Belo Horizonte, MG, Brazil

We present experimental results on the growth and structure of Fe overlayers deposited on $\text{Cu}_{84}\text{Al}_{16}(100)$ and discuss the correlation between the structural and magnetic properties of this system. Fe films 1–6 monolayers (ML) thick were grown under molecular beam epitaxy conditions onto the clean substrate at 160 K. Electron diffraction was applied to investigate the structure of the Fe films. The magnetic properties were investigated *in situ* by surface magneto-optical Kerr effect in the longitudinal geometry. Our results show that the onset of in-plane ferromagnetism around 3.5 ML of Fe coincides with structural changes that suggest a transformation within the Fe films from a fcc-like (100) to a bcc-like (110) structure with increasing Fe thickness, starting from 2.5 ML. © 2001 American Institute of Physics. [DOI: 10.1063/1.1355321]

The correlation between growth, structure, and magnetism of ultrathin Fe films on fcc substrates, particularly Cu and Cu alloys, has attracted much attention for more than a decade and even today is a matter of significant interest in surface magnetism. As demonstrated by theoretical calculations, fcc Fe (γ -Fe) should present strong magneto-volume instabilities; depending on the atomic volume the ground state of bulk metastable fcc Fe can present nonmagnetic, antiferromagnetic, or ferromagnetic (FM) high- and low-spin order.^{1–3} Moreover, the magnetic moment of FM fcc Fe atoms should increase monotonically with the lattice parameter.^{1–4} For ultrathin Fe films on Cu(100), different theoretical studies have predicted the existence of metastable spin states depending on the Fe thickness.^{5–7} Experimentally, Fe on Cu(100) is a well-studied system, which shows a complex correlation between magnetic and structural properties and these properties depend strongly on the thickness of the Fe and on the growth conditions.^{8–11} fcc Fe can also be obtained by epitaxial growth on other suitable fcc substrates to vary the expansion or contraction of the lattice parameter regarding Cu. Fe on Cu–Au alloys,^{12–15} and on Co,¹⁶ among others, represent an expansion of the lattice parameter in relation to Fe/Cu(100), and diamond (100)¹⁷ represents a contraction of the Fe lattice. We have been studying ultrathin Fe films grown on $\text{Cu}_{84}\text{Al}_{16}(100)$,^{18,19} a fcc substrate with lattice parameter of 3.65 Å, which is 1% larger than pure Cu, matches the calculated atomic volume of the ferromagnetic high-spin γ -Fe,^{1–3} and was chosen in order to favor the stabilization of that phase of fcc Fe.

In previous studies, the magnetic properties of Fe monolayers (MLs) grown on $\text{Cu}_{84}\text{Al}_{16}(100)$ were determined by linear magnetic dichroism in core level photoemission (LMDAD).^{18,19} These works have shown that Fe films (1–6 ML thick) grown at 160 K on $\text{Cu}_{84}\text{Al}_{16}(100)$ present in-plane ferromagnetism starting from ~ 2.5 ML, and that annealing at room temperature destroys the in-plane ferromag-

netic order of these Fe films in a nonreversible way.¹⁸ In these studies, the structural properties of the Fe monolayers on $\text{Cu}_{84}\text{Al}_{16}(100)$ were not sufficiently well characterized due to experimental limitations. Here, we present a complementary study on the structure and magnetism of Fe monolayers grown epitaxially at low temperature on the same $\text{Cu}_{84}\text{Al}_{16}(100)$ substrate and discuss the correlation between the structural and magnetic properties of this system. The structure of the Fe films was investigated by low energy electron diffraction (LEED) and reflection high-energy electron diffraction (RHEED), and the magnetic properties were determined by surface magneto-optical Kerr effect (SMOKE) measurements in the longitudinal geometry. The substrate temperature during Fe deposition was kept at 160 K [low temperature (LT) growth]. We investigated also changes in the structural and magnetic properties of the LT-grown films after a rapid annealing at room temperature. Results for films grown at room temperature will be published elsewhere.²⁰

All the experiments were carried out in an ultrahigh vacuum system equipped with standard techniques for preparation and analysis of thin films and surfaces including different evaporators, quartz microbalance, residual gas analyzer, x-ray photoelectron, and Auger electron spectroscopies (AES), LEED, and RHEED. The system was also equipped with instruments to measure magneto-optical Kerr effect in the longitudinal geometry *in situ* by using a diode laser beam with wavelength of 670 nm and a movable electromagnet. The base pressure in the chamber was better than 2×10^{-10} mbar. Fe overlayers (1–6 ML thick) were grown under molecular beam epitaxy conditions onto a clean $\text{Cu}_{84}\text{Al}_{16}(100)$ substrate. The surface of the substrate was previously prepared by cycles of Ar^+ sputtering at 1 keV and annealing at temperatures between 350 and 450 °C. This preparation procedure was repeated until a clean and well-ordered surface was obtained, as confirmed by AES and LEED, respectively. The Fe films were deposited from a high purity Fe wire (99.99%) which was heated by electron bombardment. The deposition rate was typically ~ 1 Å/min.

^{a)} Author to whom correspondence should be addressed; electronic mail: wmacedo@urano.cdtb.br

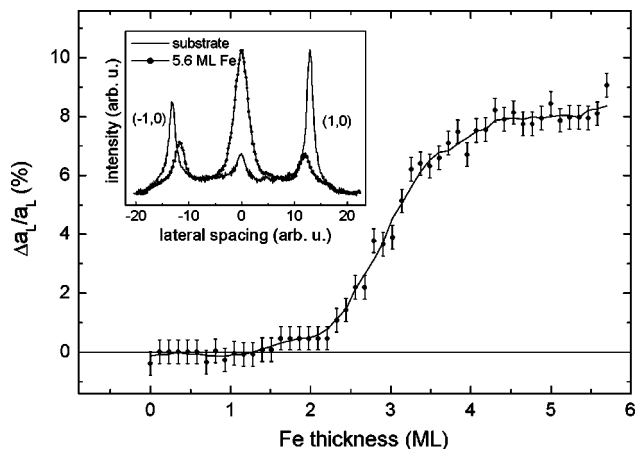


FIG. 1. Evolution of the in-plane lateral spacing during deposition of Fe on $\text{Cu}_{84}\text{Al}_{16}(001)$ at 160 K, as determined by RHEED. $\Delta a_1/a_1$ represents the variation regarding the clean substrate. (Inset) RHEED intensity profile measured perpendicular to the streaks for the clean $\text{Cu}_{84}\text{Al}_{16}(100)$ substrate and for a 5.6 ML thick Fe film, as deposited at 160 K.

The Fe films were grown at 160 K (LT). The freshly prepared Fe films were found to be free from contamination, as determined by AES. RHEED (electron energy up to 15 keV) was used to investigate the growth mode, thickness, and structure of the ultrathin Fe films. A recording system with a charge coupled device camera, a S-VHS video recorder, and a dedicated software for the data processing (EEscan) completed the RHEED setup. In this way, the electron diffraction patterns of the surface were recorded while depositing Fe, and were further analyzed. The structure of the deposited films was also investigated by intensity measurements of the LEED specular beam versus electron energy [$I(V)$ curves]. The magnetism of the Fe monolayers was investigated *in situ* by longitudinal SMOKE. Films grown at LT were submitted to a rapid annealing up to room temperature [~ 30 min of total heating time, 10 min @ room temperature (RT)] and the structural and magnetic properties were then measured again at 160 K.

Figure 1 shows a typical evolution of the in-plane lateral spacing of the Fe atoms versus films thickness during deposition at 160 K, as determined by RHEED. This spacing is obtained from the distance between two adjacent diffraction streaks in the RHEED patterns. Each point in the curve represents the relative variation of the lateral spacing in the Fe film as compared to the lateral spacing of the $\text{Cu}_{84}\text{Al}_{16}(100)$ surface (3.65 Å). As can be seen, up to about 2.5 ML Fe, the lateral spacing does not change and matches the substrate lattice parameter. Above this thickness, a progressive increase of this distance is observed and, at 4 ML of Fe, a value 8% larger than the substrate is reached. Moreover, it has been observed that the measured lateral expansion is connected to a significant change in the relative intensities of the RHEED $(\bar{1},0)$ and $(1,0)$ streaks, as shown in the inset of Fig. 1. This change suggests a small rotation in the growth direction of the Fe film, as observed for Fe on $\text{Cu}(100)$.^{10,21}

The average vertical interplanar spacing of the Fe atoms in the film was determined *in situ* by LEED after deposition. The (00) diffraction beam intensity curves were collected as

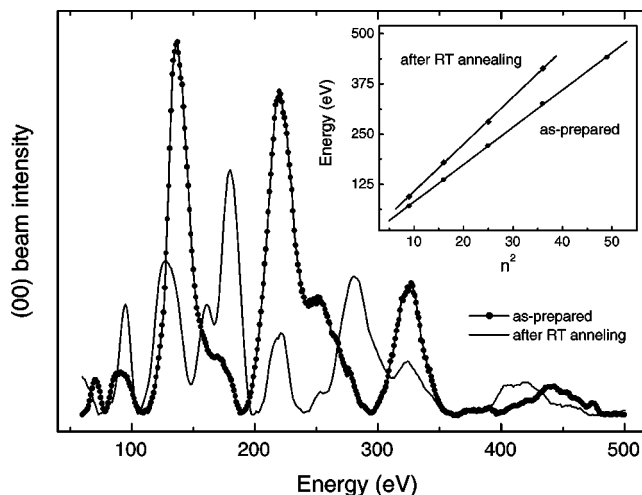


FIG. 2. LEED $I_{00}(V)$ curves for a 5.6 ML thick Fe film on $\text{Cu}_{84}\text{Al}_{16}(001)$, as deposited at 160 K, and after annealing at room temperature. The respective $E(n^2)$ curves are shown in the inset, where the straight lines represent linear regression fittings based in a kinematic approximation for the (00) diffraction beam intensity curves.

a function of the electron energy [$I_{00}(V)$ curves] after film deposition and a kinematic approximation was used to calculate the vertical interplanar distance.²² The peaks observed in the LEED $I_{00}(V)$ curves correspond to the constructive interference condition for the electron wave (Bragg condition). Considering that the electrons suffer only simple scattering in the diffraction process (the kinematic approximation), the vertical interplanar distance a_p can be evaluated by using the expression

$$a_p = n\pi\hbar / [(2m(E_p + V_0))^{1/2} \sin \theta],$$

where E_p is the primary electron energy of the Bragg peak of order n , V_0 is the additional energy shift due to the average inner potential in the crystal, m the electron mass, and θ the incident angle with respect to the sample surface. Finally, a linear fitting of the E_p versus n^2 points extracted from the $I(V)$ curves gives the vertical interplanar distance a_p .²²

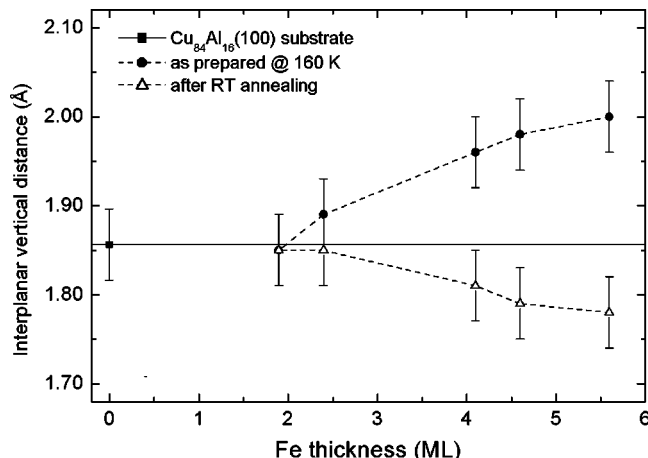


FIG. 3. Dependence of the vertical interplanar spacing vs thickness for Fe films on $\text{Cu}_{84}\text{Al}_{16}(100)$ as-deposited at 160 K (solid circles), and after annealing at room temperature (open triangles). The dashed lines are guides to the eye.

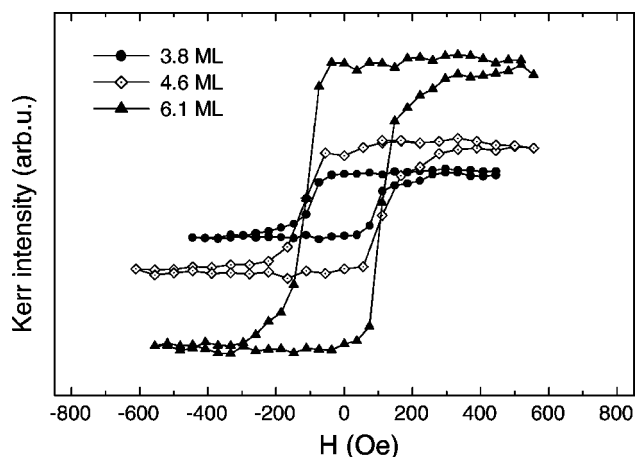


FIG. 4. Longitudinal SMOKE hysteresis loops for different ultrathin Fe films on $\text{Cu}_{84}\text{Al}_{16}(100)$, grown and measured at 140 K. No magnetic signal was measured for thicknesses ≤ 3.0 ML.

Figure 2 illustrates the determination of the vertical interplanar distances. It shows LEED $I_{00}(V)$ curves for a 5.6 ML thick Fe film on $\text{Cu}_{84}\text{Al}_{16}(100)$, as deposited at 160 K, and after annealing at room temperature, and the respective $E(n^2)$ curves (inset). In the inset, the straight lines represent linear regression fittings based in a kinematic approximation of the (00) diffraction beam intensity, as described above. These film, as-prepared, present a vertical interplanar distance of $2.00 \pm 0.05 \text{ \AA}$, and after RT annealing the vertical spacing decreases to $1.80 \pm 0.05 \text{ \AA}$.

The dependence of the vertical interplanar spacing as a function of the film thickness for as-deposited and annealed films is displayed in Fig. 3 (circles). For as-deposited films, the LEED $I(V)$ results show a linear increase of the interplanar spacing with Fe thickness reaching a value 8% larger than the lattice parameter of the $\text{Cu}_{84}\text{Al}_{16}(100)$ substrate for 5.6 ML. It must be observed that this structural evolution resembles the evolution of the lateral spacing with increasing Fe thickness, shown in Fig. 1, and it is evidence of a structural transformation within the Fe films during the growth at low temperature. The RHEED and LEED results, i.e., the lattice expansion and the small rotation in the growth direction suggest that, for low temperature growth starting from 2.5 ML, as the Fe thickness increases up to ~ 5 ML the structure of the Fe film changes from fcc like [100] to a bcc like [110], similar to the observed for the growth of Fe on $\text{Cu}(100)$ at low temperature.¹⁰

Effects of annealing at room temperature on the in-plane lateral and interplanar distances of Fe films deposited at 160 K were also investigated by RHEED and LEED measurements. By annealing, the Fe films preserve the lateral spacing (within $\pm 2\%$) and a clear contraction of the interplanar spacing is observed, to a distance very close to that of the $\text{Cu}_{84}\text{Al}_{16}(100)$ substrate, as shown in Fig. 3 (open triangles).

The in-plane ferromagnetism of the ultrathin Fe films (0.8 and 6.1 ML thick) grown on $\text{Cu}_{84}\text{Al}_{16}(100)$ at low temperature was investigated *in situ* by longitudinal SMOKE.²³ Starting from ~ 3.5 ML, a clear square hysteresis loop can be observed. Figure 4 shows typical longitudinal SMOKE loops for the Fe films on $\text{Cu}_{84}\text{Al}_{16}(100)$, measured at 140 K immediately after deposition, in an applied magnetic field up to 600 Oe, as calibrated with a Hall probe. The MOKE intensity increases linearly with Fe thickness while the coercivity remains constant, around 100 Oe. For thickness > 3.5 ML, the ultrathin Fe films on $\text{Cu}_{84}\text{Al}_{16}(100)$ are ferromagnetic, with in-plane easy axis, in agreement with previous LMDAD results.¹⁸ Moreover, by comparing Figs. 1 and 4, our results show that the onset of in-plane ferromagnetism in LT-grown films is clearly connected to the onset of expansion of the lateral spacing, i.e., to the onset of distortion of the fcc-like structure. After annealing at RT, no magnetic loop has been obtained at LT, presumably due to the observed interplanar contraction and to Al interdiffusion.¹⁸

The authors gratefully acknowledge the financial support of the Brazilian Agencies CNEN, CNPq, and FAPEMIG.

- ¹V. L. Moruzzi, P. M. Marcus, and J. Kübler, *Phys. Rev. B* **39**, 6957 (1989), and references therein.
- ²T. Kraft, P. M. Marcus, and M. Scheffler, *Phys. Rev. B* **49**, 11511 (1994).
- ³M. Uhl, L. M. Sandratskii, and J. Kübler, *J. Magn. Magn. Mater.* **103**, 314 (1992).
- ⁴D. Guenzburger and D. E. Ellis, *Phys. Rev. B* **51**, 12519 (1995).
- ⁵T. Asada and S. Blügel, *Phys. Rev. Lett.* **79**, 507 (1997).
- ⁶R. Lorenz and J. Hafner, *Phys. Rev. B* **58**, 5197 (1998).
- ⁷P. M. Marcus, V. L. Moruzzi, and S.-L. Qiu, *Phys. Rev. B* **60**, 369 (1999).
- ⁸D. Li, M. Freitag, J. Pearson, Z. Q. Qiu, and S. D. Bader, *Phys. Rev. Lett.* **72**, 3112 (1994).
- ⁹R. D. Ellerbrock, A. Fuest, A. Schatz, W. Keune, and R. A. Brand, *Phys. Rev. Lett.* **74**, 3053 (1995).
- ¹⁰S. Müller, P. Bayer, C. Reischl, K. Heinz, B. Feldmann, H. Zillgen, and M. Wuttig, *Phys. Rev. Lett.* **74**, 765 (1995).
- ¹¹W. A. A. Macedo and W. Keune, *Phys. Rev. Lett.* **61**, 475 (1988).
- ¹²F. Baudelet, M.-T. Lin, W. Kuch, K. Meinel, B. Choi, C. M. Schneider, and J. Kirschner, *Phys. Rev. B* **51**, 12563 (1995); M.-T. Lin, J. Shen, W. Kuch, H. Jenniches, M. Klaua, C. M. Schneider, and J. Kirschner, *ibid.* **55**, 5886 (1997).
- ¹³R. Rochow, C. Carbone, Th. Dodt, F. P. Johnen, and E. Kisker, *Phys. Rev. B* **41**, 3426 (1990).
- ¹⁴W. A. A. Macedo, W. Keune, and R. D. Ellerbrock, *J. Magn. Magn. Mater.* **93**, 552 (1991).
- ¹⁵D. J. Keavney, D. F. Storm, J. W. Freeland, I. L. Grigorov, and J. C. Walker, *Phys. Rev. Lett.* **74**, 4531 (1995).
- ¹⁶W. L. O'Brien and B. P. Tonner, *Surf. Sci.* **334**, 10 (1995).
- ¹⁷D. Li, D. J. Keavney, J. Pearson, S. D. Bader, J. Pege, and W. Keune, *Phys. Rev. B* **57**, 10004 (1998).
- ¹⁸W. A. A. Macedo, F. Sirotti, G. Panaccione, A. Schatz, W. Keune, W. N. Rodrigues, and G. Rossi, *Phys. Rev. B* **58**, 11534 (1998).
- ¹⁹W. A. A. Macedo, F. Sirotti, A. Schatz, D. Guarisco, G. Panaccione, W. Keune, and G. Rossi, *J. Magn. Magn. Mater.* **177-181**, 1262 (1998).
- ²⁰M. D. Martins and W. A. A. Macedo (unpublished).
- ²¹H. Zillgen, B. Feldmann, and M. Wuttig, *Surf. Sci.* **321**, 32 (1994).
- ²²J. B. Pendry, *Low Energy Electron Diffraction* (Academic, New York, 1974).
- ²³Z. Q. Qiu and S. D. Bader, *J. Magn. Magn. Mater.* **200**, 664 (1999).